World Academy of Science, Engineering and Technology
International Journal of Chemical and Molecular Engineering
Vol:3, No:9, 2009

Molecular Dynamics Simulation of Liquid-Vapor Interface on the Solid Surface Using the GEAR'S Algorithm

D. Toghraie, and A. R. Azimian

***Abstract*—**In this paper, the Lennard -Jones potential is applied to molecules of liquid argon as well as its vapor and platinum as solid surface in order to perform a non-equilibrium molecular dynamics simulation to study the microscopic aspects of liquid-vapor-solid interactions. The channel is periodic in x and y directions and along z direction it is bounded by atomic walls. It was found that density of the liquids near the solid walls fluctuated greatly and that the structure was more like a solid than a liquid. This indicates that the interactions of solid and liquid molecules are very strong. The resultant surface tension, liquid density and vapor density are found to be well predicted when compared with the experimental data for argon. Liquid and vapor densities were found to depend on the cutoff radius which induces the use of $P3M$ (particle-particle particle-mesh) method which was implemented for evaluation of force and surface tension.

***Keywords*—**Lennard-Jones Potential, Molecular Dynamics Simulation, Periodic Boundary Conditions (PBC), Non-Equilibrium Molecular Dynamics (NEMD**)**.

I. Introduction

SIMULATION of micro scale thermo-fluidic transport has attracted considerable attention in recent years owing to rapid advances in microelectronic fabrication technologies and the promise of emerging nano-technologies.

Molecular dynamics MD has emerged as a powerful technique to model the fluid flow studies with linear dimensions of the order of a few hundred nanometers or less for typical simulation runs lasting hundreds of picoseconds. Molecular dynamic method is employed aiming to get a microscopic insight into the complex liquid - vapor -solid system. Molecular simulation is a statistical mechanics method to achieve a set of configurations distributed according to a statistical ensemble. NEMD involves the simulation of a classical N-body system of atoms or molecules interacting via interatomic potential forces. However, in addition to interatomic forces, an external field drives the system away from thermodynamic equilibrium.

D. Toghraie is with the Isfahan University of Technology, Isfahan, Iran (corresponding author to provide phone: 0098-913-322-1167; fax: 0098-311-2238384; e-mail: davoodtoghraie@ gmail.com).

A.R.Azimian is with the Isfahan University of Technology, Isfahan, Iran (e-mail: azimian@cc.iut.ac.ir).

Since the walls couple to the environment that is possibly in thermal equilibrium, while the fluid in the channel is not. In these situations, often a constant temperature condition can be desirable, which requires the dissipation of the excess energy. For systems in equilibrium, molecular dynamics has emerged as the dominant simulation technique at the atomic scale. The main idea behind classical MD is the calculation of the interactions between atoms and the solution of Newton's equations of motion for each particle in order to extract thermodynamic properties, such as pressure and transport properties, like shear viscosity, bulk viscosity, thermal conductivity, etc. It should be noted that the external applied force (for walls) induces an amount of energy to the system, which may lead to non-linearity. As the force magnitude increases, the flow becomes too fast, the system's response becomes non-linear and strong temperature variations appear. In addition, the flow reaches nonlinearities if one keeps the force constant and simply increases the channel width. For this reason, the amplitudes of the external applied forces vary in this work, depending on the width of the channel under examination. In molecular dynamics simulations several ways of thermostatting a system exist [1]-[7] some of these are velocity rescaling, Nose Hoover or Anderson thermostats, and the use of velocity-and/or position-dependent forces. Ohara and Suzuki [8] simulated numerically liquid argon (without vapor phase) between two solid walls and studied the intermolecular energy transfer at the solid-liquid interface. Yi [9] carried out molecular dynamics simulations of vaporization phenomena of an ultra-thin layer of argon on a platinum surface. They simulated the whole vaporization process for two temperature cases and also the reverse process lays condensation, after complete evaporation. Recently, while simulating an argon system, Sinha [10], [11] found that truncating long-range terms of the Lennard-Jones potential function at 4.5σ would cause errors as high as 15 percent in surface tension, which can be eliminated by using the Particle-Particle-Particle-Mesh ($P3M$) method for long range terms. They also suggested that the long-range interaction of the Lennard-Jones term in SPC/E model of water was not negligible. The well-known model used in MD includes the Lennard-Jones fluids that interact, with each other via the Lennard-Jones potential.

The overall aims of this paper are to get a microscopic

insight into the complex liquid-vapor-solid system and a fundamental understanding of the physical mechanism, which will be beneficial for the development of a phase change phenomena.

II. Simulation Procedure

The fluid molecules have been assumed to be constitutes of quantities of spherical molecules. Newton's second law is considered to be valid to describe the molecular motion in the system. Hence:

$$m_i \frac{d^2 r_i}{dt^2} = \sum_{i \neq j} F_{ij} + F_{long-range} + F_{External} = -\frac{\partial u(r_{ij})}{\partial r_i} + F_{External} + F_{long-range} \quad (1)$$

Where r_{ij} is the intermolecular potential, $F_{external}$ is an external force (for Walls) that drives the system away from the thermodynamic equilibrium and $F_{long-range}$ is a smoothly varying part and has a Fourier transform which is band-limited and can be represented on mesh. This long range part is non-zero in Fourier space and is approximated by particle-mesh (PM) method. In this study, we simulate by the well-known 12-6 Lennard Jones potential:

$$u(r_{ij}) = \left\{ 4\varepsilon \left[\left(\frac{\sigma}{r_{ij}} \right)^{12} - \left(\frac{\sigma}{r_{ij}} \right)^{6} \right] \right\} \qquad r_{ij} \le r_c \quad (2)$$

Where ε is the interaction strength (energy), σ is the (typical) diameter of the particles and r_c is the cut-off radius beyond which the intermolecular interaction could be ignored. This potential represents the important short-range repulsive interactions in the fluid. It has a zero value and a zero gradient at the point of truncation, which assists energy conservation in MD simulations. Hence, for the purpose of physical understanding, in the present study, argon is used as the LJ fluid with the following potential parameters: $m_l = 6.63 \times 10^{-26} kg$, $\sigma_l = 0.3045 nm$, $\varepsilon_l = 1.67 \times 10^{-21} J$. The potential function between the solid and liquid molecules is represented by Lennard -Jones function as:

$$u_{wall}(z) = \left\{ 4\alpha\varepsilon_{Sl} \left[\left(\frac{\sigma_{Sl}}{z} \right)^{12} - \beta \left(\frac{\sigma_{Sl}}{z} \right)^{6} \right] \right\} \quad (3)$$

$$\varepsilon_{Sl} = \sqrt{\varepsilon_S \varepsilon_l} \quad , \quad \sigma_{Sl} = \frac{\sigma_S + \sigma_l}{2}$$

Where, the Lorentz–Berthelot mixing rules are applied to the system. Here, α and β were set to 1 to simplify the calculations. The solid wall is represented by three layers of face centered cubic FCC (111) surface of platinum molecules with parameters as $m_s = 3.24 \times 10^{-26} kg$, $\sigma_s = 2.475 A^{\circ}$ and $\varepsilon_s = 8.35 \times 10^{-20} J$. The effect of the (artificial) thermostats on the dynamics of the systems is examined. For velocity rescaling, the velocities are first updated from the forces acting on the particles and then rescaled at each time step according to:

$$v_i^{new} = v_i^{old} \sqrt{\frac{T_{desired}}{T_{actual}}} \quad (4)$$

Where $T_{desired}$ is the target temperature and T_{actual} the instantaneous (global) temperature of all fluid particles in the system. The temperature is defined here as fluctuation kinetic energy (the mean velocity has to be disregarded) per particle, per degree of freedom:

$$T = \frac{\sum_{i=1}^{N_{atm}} m \left({v_{xi}}^2 + {v_{yi}}^2 + {v_{zi}}^2 \right)}{3 k_B N_{atm}} \quad (5)$$

Where k_B is the Boltzmann constant and N_{atm} is the number of atoms. The velocity Gears Predictor-Corrector Algorithm [14] is used to solve the equation of motion in the present study, due to its numerical stability, convenience and simplicity,

$$r(t+\delta t) = r(t) + \dot{r}(t)\delta t + \frac{1}{2}\ddot{r}(t)(\delta t)^2 + \frac{1}{6} r^{(iii)}(t)(\delta t)^3 + \frac{1}{24} r^{(iv)}(t)(\delta t)^4 + \frac{1}{120} r^{(v)}(\delta t)^5 \quad (6)$$

$$\dot{r}(t+\delta t) = \dot{r}(t) + \ddot{r}(t)\delta t + \frac{1}{2} r^{(iii)}(t)(\delta t)^2 + \frac{1}{6} r^{(iv)}(t)(\delta t)^3 + \frac{1}{24} r^{(v)}(t)(\delta t)^4 \quad (7)$$

$$\ddot{r}(t+\delta t) = \ddot{r}(t) + r^{(iii)}(t)\delta t + \frac{1}{2} r^{(iv)}(t)(\delta t)^2 + \frac{1}{6} r^{(v)}(t)(\delta t)^3 \quad (8)$$

$$r^{(iii)}(t+\delta t) = r^{(iii)}(t) + r^{(iv)}(t)\delta t + \frac{1}{2} r^{(v)}(t)(\delta t)^2 \quad (9)$$

$$r^{(iv)}(t+\delta t) = r^{(iv)}(t) + r^{(v)}(t)\delta t \quad (10)$$

$$r^{(v)}(t+\delta t) = r^{(v)}(t) \quad (11)$$

$$\Delta \ddot{r} = \left[\ddot{r}(t+\delta t) - \ddot{r}^{\,p}(t+\delta t) \right] \quad (12)$$

$$r = r^p + \alpha_0 \Delta R \quad (13)$$

$$\dot{r} = \dot{r}^{\,p} + \alpha_1 \Delta R \quad (14)$$

$$\ddot{r} = \ddot{r}^{\,p} + 2\alpha_2 \Delta R \quad (15)$$

$$r^{(iii)} = r^{(iii)P} + 6\alpha_3 \Delta R \quad (16)$$

$$r^{(iv)} = r^{(iv)P} + 24\alpha_4 \Delta R \quad (17)$$

$$r^{(v)} = r^{(v)P} + 120\alpha_5 \Delta R \quad (18)$$

$$\Delta R = \frac{\Delta \ddot{r}(\delta t)^2}{2} \quad (19)$$

Where, $\alpha_i (i = 1,2,3,4,5)$ are listed in Tables I.

TABLE I
THE VALUES OF $\alpha_i (i = 1, 2, 3, 4, 5)$

α_i	α_0	α_1	α_2	α_3	α_4	α_5
value	3/16	251/360	1	11/18	1/6	1/60

Initial velocities of atoms are specified randomly from a Gaussian distribution based on the specified temperature using the following formula:

$$\frac{1}{N_{atm}} \sum_{i=1}^{N_{atm}} \frac{1}{2} m \left| v_i^2 \right| = \frac{3}{2} k_B T \quad (20)$$

The velocity and temperature profiles are obtained by binning the atomic positions in 50 slabs parallel to the walls. Tracking the particles passing in each slice, the value for velocity and temperature have been calculated by averaging the data recorded for all samples. After achieving a steady state condition from the initial state, the equilibrium system properties are sampled in the micro-canonical ensemble (constant number of atom, volume and temperature).

III. Methods and Materials

In a MD simulation involving phase equilibrium, a density is required to differentiate between liquid-vapor phases. In case of a liquid-vapor interface parallel to xy plane, density is evaluated as a function of z by dividing the field into N_{bin} number of rectangular slabs of thickness Δz. If N_{zi} is the number of molecules in i_{th} bin of step j, N_{sample} is the number of sampling and m is the mass of molecules, then the density is given through the following equation:

$$\rho(z) = \frac{N_{zi} m}{N_{sample} L_x L_y \Delta z} \quad (21)$$

Where L_x and L_y are the box lengths along x and y directions, respectively. At the atomic scale, the surface tension can be expressed as the integrated imbalance of normal and tangential pressure near the interface. The following expressions are used to calculate the two components of the pressure tensor,

$$p_T(z) = k_B T \langle \rho(z) \rangle - \frac{1}{\forall} \left\langle \sum_{i=1}^{N_{atm}-1} \sum_{j=i+1}^{N_{atm}} \frac{(y_{ij}^2 + x_{ij}^2) u'_{ij}}{2 r_{ij}} \right\rangle \quad (22)$$

$$p_N(z) = k_B T \langle \rho(z) \rangle - \frac{1}{\forall} \left\langle \sum_{i=1}^{N_{atm}-1} \sum_{j=i+1}^{N_{atm}} \frac{(z_{ij})^2 u'_{ij}}{2 r_{ij}^2} \right\rangle - \sum_{i=1}^{N_{atm}} \frac{z_i u'_{wall}(z)}{\forall} \quad (23)$$

Where $\langle\ \rangle$ denotes an ensemble average taken over the duration of the simulation for which thermal equilibrium exists. In terms of atomic position and liquid-vapor potential u and solid potential u_{wall}, the expression for surface tension is:

$$\gamma_{lv} = \int_{-\infty}^{+\infty} [P_N(z) - P_T(z)] dz = \left\langle \sum_{j=1}^{N_{atm}-1} \sum_{i=j+1}^{N_{atm}} \frac{x_{ij}^2 + y_{ij}^2 - 2z_{ij}^2}{2Ar_{ij}} u'_{ij} - \sum_{j=1}^{N_{atm}} \frac{z_j u'_{wall}(z)}{A} \right\rangle \quad (24)$$

IV. Result and Discussion

In the first case of simulations, the simulation was performed for slab geometry. The simulation domain was a triply periodic rectangular box with dimensions $L_x = 12\sigma_l$, $L_y = 12\sigma_l$ and $L_z = 24\sigma_l$. Periodic boundary conditions are applied to all three directions. The initial condition was to assume a liquid slab in the central region of the z direction of the simulation box. The temperature of all argon atoms are set at the saturated temperatures. Density profile of the Lennard - Jones atoms in the direction normal to the interface is shown in Fig. 1.

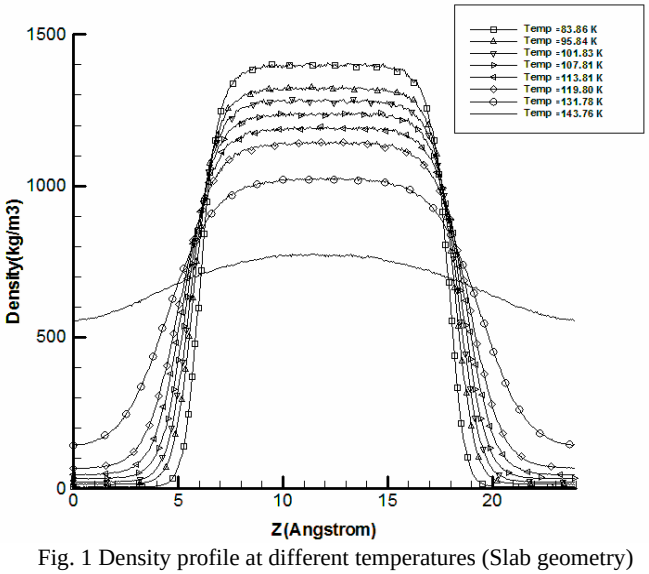

Fig. 1 Density profile at different temperatures (Slab geometry)

It is clear from the profiles that a well defined interface is founded and pure liquid and vapor regions exist on different sides. Liquid and vapor densities are obtained from it and are plotted in Fig. 2. These values are compared with the density of argon fluid from experiments [12] and [13] [see Fig. 2 and Table II] and the results obtained from Verlet Algorithm. It is

clear that the simulations predict liquid and vapor densities quit well. As temperature increases, liquid density decreases and vapor density increases and the difference vanishes near the critical point $(151K)$.

The surface tension dependence on the system temperature is shown in Fig. 3. It is possible to see that the liquid-vapor surface tension drops with increasing temperature. Also simulation results are compared with thermodynamic correlations based on the principle of the corresponding states for the surface tension of argon in this figure. Numerical results obtained were in good agreements with the experimental data. In the second case Molecular dynamics simulations are performed for liquid molecules were set on the solid wall on the z-axis.

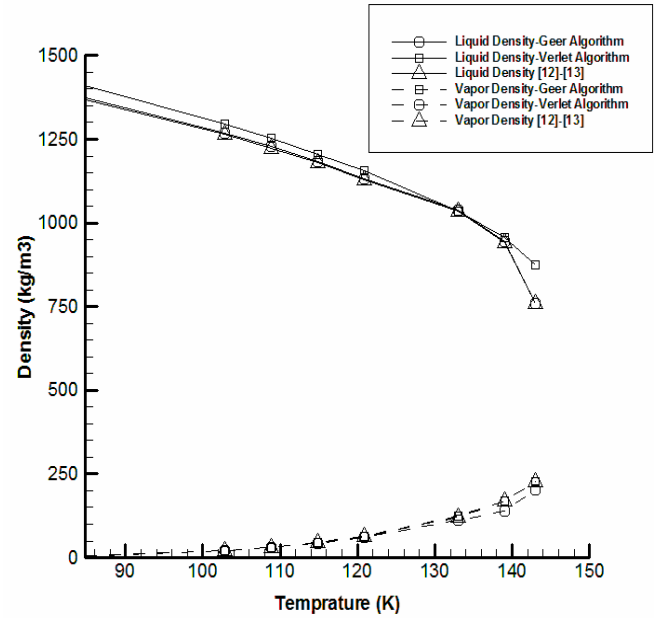

Fig. 2 Liquid and vapor densities versus temperature for both Verlet and Geer Algorithm

TABLE II
LIQUID DENSITY AND VAPOR DENSITY OF ARGON WITH GEER'S ALGORITHM

$T_{sat}(K)$	$\rho_g(kg/m^3)$		$\rho_f(kg/m^3)$	
	Simulation results for $\frac{r_c}{\sigma}=4$	References [12],[13]	Simulation results for $\frac{r_c}{\sigma}=4$	References [12],[13]
84.80	4.96	4.524	1373	1368.19
102.7	20.96	20.790	1269	1265.47
108.8	31.11	31.055	1227.5	1224
114.8	44.96	44.843	1182.9	1180.5
120.9	63.95	63.694	1132	1129.77
133.0	123.12	123.45	1038	1035.05
139	169.86	169.49	943.5	940

The simulation domain consists of 1400 liquid molecules. The simulation cell has the size of $L_x = 12\sigma_l, L_y = 12\sigma_l$ and $L_z = 24\sigma_l$ The solid wall consists of one layer of platinum molecules organized as a FCC lattice surface in contact with the liquid. Periodic boundary conditions with respect to the number of molecules are applied along the x- and y-directions and mirror boundary condition at $z = L_z$. The domain between the wall surface and the upper boundary of the computational domain is divided into 512 equal slices.

Fig. 4 shows the density profiles of argon in the direction normal to the interface in the equilibrium conditions (at saturated temperature) in which external force of the wall was applied. It is shown that the liquid molecules in the snapshots are distributed orderly in the neighborhood of the solid interface due to strong solid–liquid interactions. The experimental and simulation results for specific volume of the two phase equilibrium parameters of Argon (liquid and vapor) are listed in Table III and Table IV.

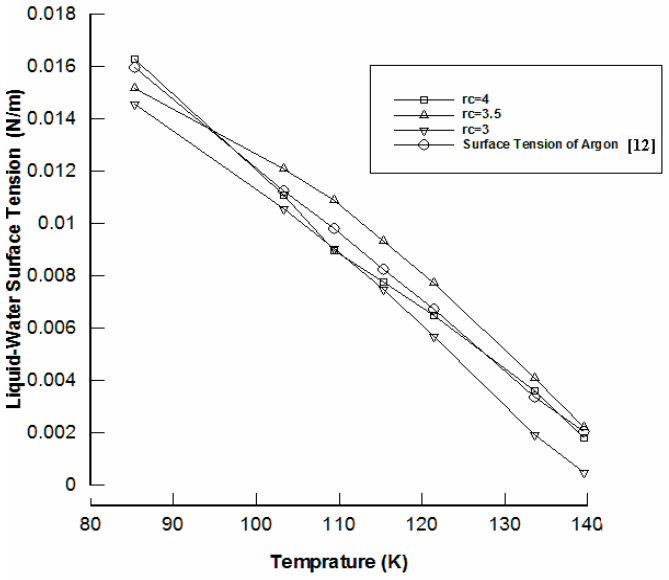

Fig. 3 Surface temperature versus temperature

Results are in good agreement with the data in CATT2 [12], the maximum error is not more than 4% for $r_c = 4\sigma$. This indicated that the neighbor list method with a finite cutoff radius is good for short range term of the Lennard-Jones potential and $P3M$ method is much better for evaluating the long range term of the Lennard-Jones potential for simple fluids such as argon.

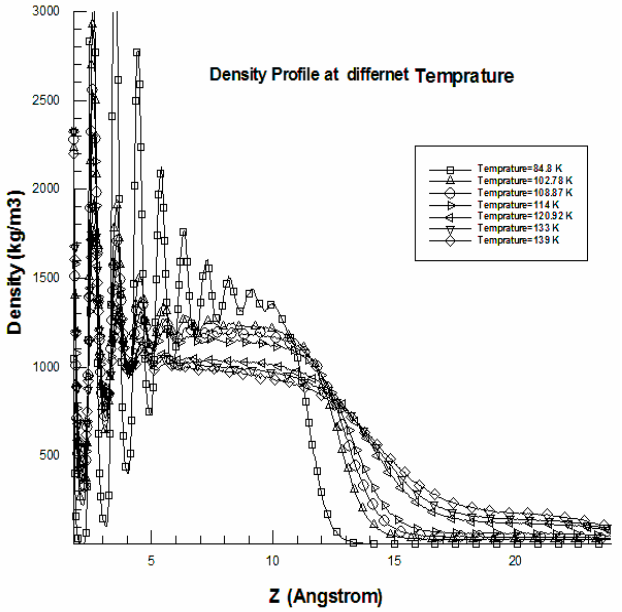

Fig. 4 Density profile at different temperatures (Solid geometry)

TABLE III
SPECIFIC VOLUME OF LIQUID ARGON (GEER'S ALGORITHM)

$T_{sat}(K)$	Simulation results $\frac{r_c}{\sigma}=3$	Simulation results $\frac{r_c}{\sigma}=3.5$	Simulation results $\frac{r_c}{\sigma}=4$	References [12],[13]
84.8	0.00075	0.00072	0.000705	0.00070
102.7	0.0008	0.00078	0.000775	0.00077
108.8	0.00082	0.00081	0.000804	0.00079
114.8	0.00084	0.000829	0.000826	0.00082
120.9	0.0009	0.00089	0.000869	0.00086
133.0	0.00119	0.00103	0.00096	0.00096
139	0.00136	0.00129	0.001049	0.00104

TABLE IV
SPECIFIC VOLUME OF VAPOR ARGON (GEER'S ALGORITHM)

$T_{sat}(K)$	Simulation results $\frac{r_c}{\sigma}=3$	Simulation results $\frac{r_c}{\sigma}=3.5$	Simulation results $\frac{r_c}{\sigma}=4$	References [12],[13]
84.8	0.140	0.195	0.22	0.22
102.7	0.036	0.0412	0.0469	0.048
108.8	0.029	0.0305	0.0316	0.032
114.8	0.017	0.0196	0.021	0.022
120.9	0.011	0.013	0.0142	0.015
133.0	0.0061	0.0074	0.0079	0.008
139	0.0041	0.0044	0.00495	0.005

V. CONCLUSION

In this work, numerical simulations based on the non-equilibrium molecular dynamics are performed to investigate liquid-vapor-solid system. The liquid-vapor-solid system is studied by changing the cutoff radius, saturation temperature and the number of fluid molecules. The results show that as temperature increases, liquid density decreases and vapor density increases and the difference vanishes near the critical point. Also, Surface tension decreases with increasing temperature.

REFERENCES

[1] M. P. Allen, D. J. Tildesley, *Computer simulation of liquids,* New York: Oxford University Press Inc., 1987.
[2] J. Koplik, J. R. Banavar, "Molecular dynamics simulation of microscale Poiseuille flow and moving contact lines", Phys. *Rev. Lett,* vol. 60, pp. 1282-1285, 1988.
[3] P. A. Thompson, M. O. Robbins, "Shear flow near a solid: Epitaxial order and flow boundary condition", *Phys. Rev. A,* vol. 41, pp. 6830, 1990.
[4] Bitsanis, Ioannis, Somers, Susan A., H. Ted Davis, and MathewTirrel, "Molecular Dynamics of flow in molecularly arrow pore", *J. Chem. Phys.,* vol. 93, pp. 3427-3436, 1990.
[5] X. J. Fan, N. Phan Thien, N. T. Tong and X. Diao, "Molecular dynamics simulation of a complex channel flow", *Physics of Fluids,* vol. 14, pp. 114-120.
[6] J. Eggers, "Dynamics of a nanojet", *Phys. Rev. Lett, Vol.* 89, pp.084502-084510, 2002.
[7] E. Rudd Rober, Q. Broughton Jeremy, "Coarse-grained molecular dynamics and the atomic limits of finite elements", *Phys. Rev. B,* vol. 58, pp. 5893-5600, 1998.
[8] T. Ohara, D. Suzuki, "Intermolecular energy transfers at a solid–liquid interface", *Micro scale Thermo physical Engineering*, vol. 4, pp. 189–196, 2000.
[9] P. Yi, D. Poulikakos, J. Walther, G. Yadigaroglu, "Molecular dynamics simulation of vaporization of an ultra-thin liquid argon layer on a surface", *Int. J. Heat Mass Tran.*, vol. 45, pp. 2087–2100, 2002.
[10] S. Sinha, V. K. Dhir, J. B. Freund and E. Darve, "Fast truncation-free method for dispersive attractions in a molecular dynamics simulation", *Journal of Computational Physics*, 2006.
[11] . Sinha, B. Shi, V. K. Dhir, J. Freund, and E. Darve, "Surface tension evaluation in lennard-jones fluid system with untruncated potentials", *In Proceedings of 2003 ASME Summer Heat Transfer Conference*, 2003.
[12] W. C. Reynolds, *Thermodynamic Properties in SI*, Stanford University Press, 1979.
[13] "Computer Aided Thermodynamics Table 2", Version 1.a, Copyright© 1996, by John Wiley & Sons, Inc.
[14] J. M. Hail, *molecular dynamics Simulation, Elementary methods*, john Wiley & Sons, INC, 1992.